## HELIUM25 - Helium burning and perspectives for underground labs

21–25 lug 2025
Helmholtz-Zentrum Dresden-Rossendorf (HZDR)

Roberta Spartà

# Helium burning with Trojan Horse method

# The need of indirect methods



to measure cross sections at energies never reached / reached but with very large uncertainties

to retrieve information on electron screening effect when ultra-low energy measurements are available    *Plasma screening ≠ Lab screening*
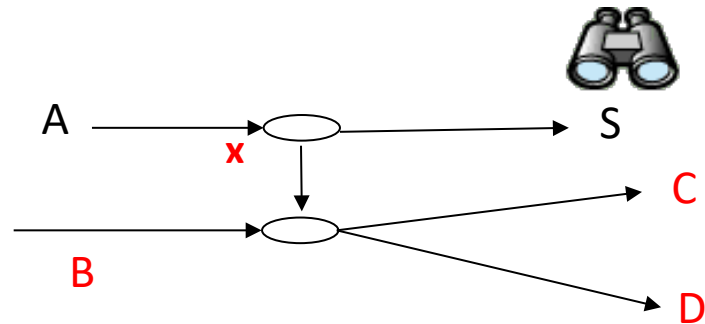
***complementary to the direct ones***

# THM description: overcoming the CB

Main idea: to get the 2-body reaction σ
<u>selecting the quasi-free mechanism</u>
from the σ of a properly chosen 3-body reaction

A+B→C+D+S
The 3-body reaction you perform in the lab
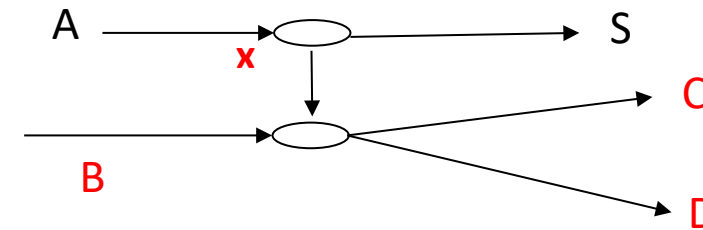
A is the Trojan Horse nucleus
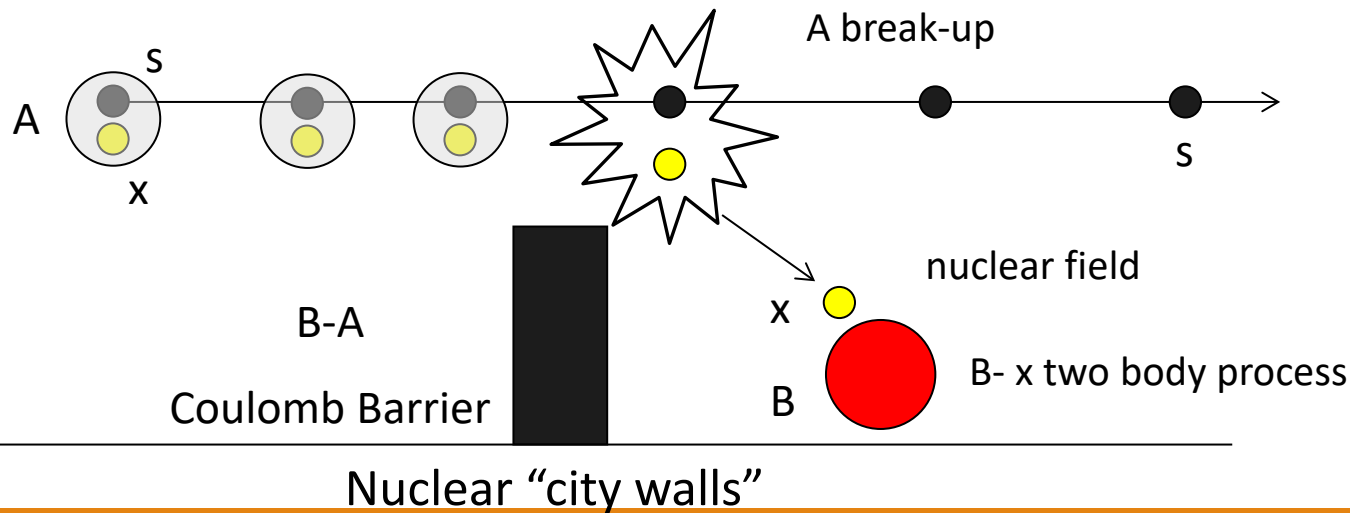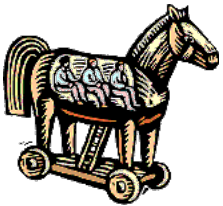
$$x \oplus S$$



x+B→C+D
The binary reaction of interest

# THM description: overcoming the CB

$E_A > (E_{AB})_{Coulomb\ Barrier}$

The nucleus A can be brought into nuclear field of nucleus B and the cluster x induces the reaction

$x + B \rightarrow C + D$

A ———→ ○ ———————→ S
       x
                    ○ ———→ C
B ———————————→          D

Trojan Horse nucleus

A break-up

S
A
x

B-A

Coulomb Barrier

Nuclear "city walls"

nuclear field

x
B    B- x two body process

s

Coulomb effects and electron screening are negligible

# THM description: going to low energies

$$E_{qf} = E_{xB} - B_{x-S} = E_{cD} - Q_{2b}$$

$E_{xB}$ is the beam energy in the center of mass of the two body reaction

$B_{x-S}$ binding energy of the two clusters inside the Trojan Horse

*plays a key role in compensating for the beam energy*

*under proper kinematical conditions*

# THM description: QF mechanism

QF mechanism: the spectator in the exit channel keeps the same momentum inside the TH nucleus.

In **PWIA** the cross section of the 3-body reaction can be factorized in two terms corresponding to the two vertices

First vertex

virtual decay of nucleus A->x+S

Second vertex

virtual reaction    x+B→C + D

$$\frac{d^3\sigma}{dE_C d\Omega_C d\Omega_D} \propto KF[F(q)_{xS}]^2 \left[\frac{d\sigma}{d\Omega}\right]^{TH}_{x+B\to C+D}$$

kinematical factor

$|F(q_{xS})|^2$ describes the intercluster (x-S) momentum distribution
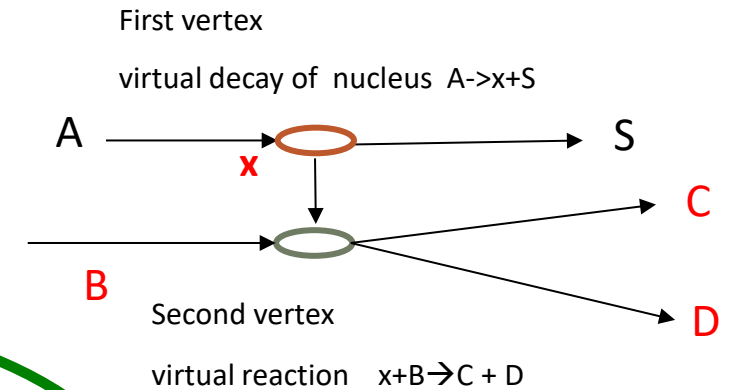
# THM description: direct-indirect σ

*THM no absolute cross section → Normalization to direct measurements at higher energies*

*(main validity test)*

Excitation function

**ABOVE** COULOMB BARRIER

$$\left[\frac{d\sigma}{dE,d\Omega}\right]^{TH\ (HOES)}_{x+B\to C+D} \propto \left[\frac{d\sigma}{dE,d\Omega}\right]^{Direct\ (OES)}_{x+B\to C+D}$$

**BELOW** COULOMB BARRIER

$$\left[\frac{d\sigma}{dE,d\Omega}\right]^{TH\ (HOES)}_{x+B\to C+D} * \sum P_l \propto \left[\frac{d\sigma}{dE,d\Omega}\right]^{Direct\ (OES)}_{x+B\to C+D}$$

$$P_l(q_{ax}) = \frac{1}{G_l^2(k_{ax}R) + F_l^2(k_{ax}R)}$$
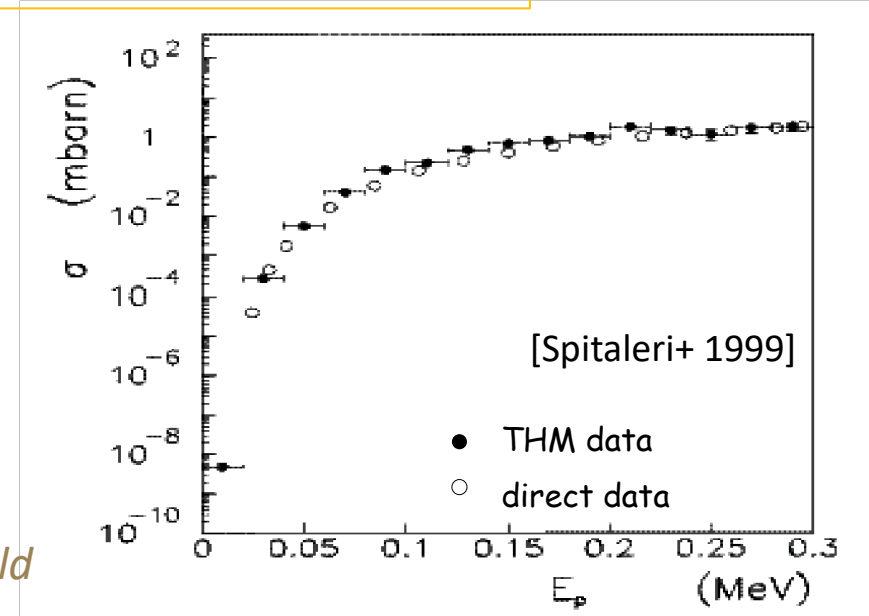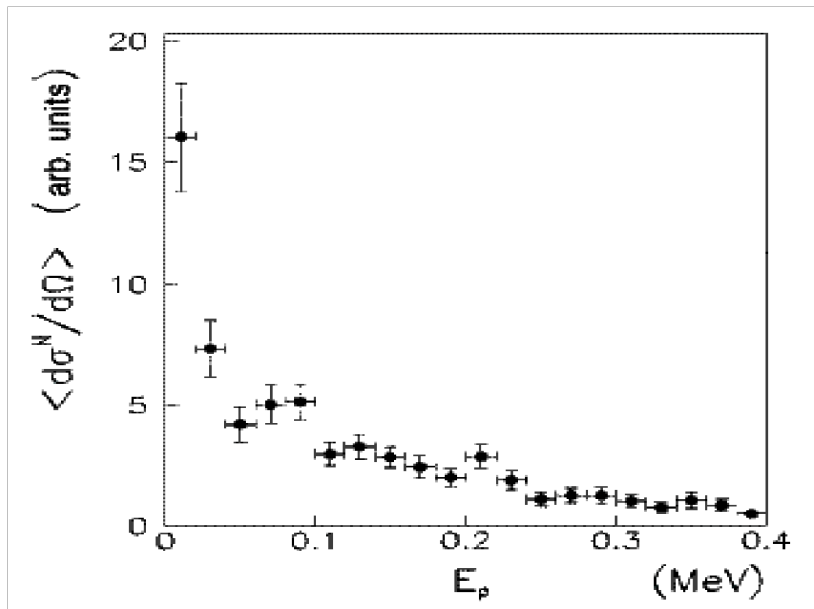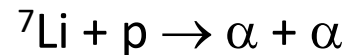
# THM description: direct-indirect σ

$$\left[\frac{d\sigma}{dE,d\Omega}\right]_{x+B\rightarrow C+D}^{TH\ (HOES)} * \sum P_l \propto \left[\frac{d\sigma}{dE,d\Omega}\right]_{x+B\rightarrow C+D}^{Direct\ (OES)}$$



[Spitaleri+ 1999]

● THM data

○ direct data

#oldbutgold

$^7$Li + p → α + α

# Other approaches – Modified PWBA

From DWBA: surface approximation…→ "Modified Plane Wave Born Approximation"
for non resonant reactions [Typel et al. 2000], [Typel et al. 2003] …

DWBA (Distortions are introduced in the c+C channel while Plane Waves hold for the 3-body
entrance/exit channel )→ surface approximation (only peripheral reactions are considered)

$$\frac{d^3\sigma}{dE_C d\Omega_C d\Omega_c} \propto KF' \left| W(\vec{Q}_{Bs}) \right|^2 \frac{v_{Cc}}{k_{Cc}^2 Q_{Aa}^2 v_{ax}} \sum_l \left( \frac{d\sigma_l}{d\Omega} \right)_{ax \to Cc}$$

$$Q_{Bs} = k_{Bs}^f - k_{Aa}^i \frac{m_s}{m_x + m_s}$$

A ————————————→ s

x

a ————————————→ c

C
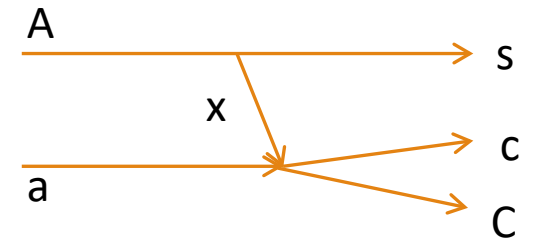
# Other approaches – Modified R-matrix

**Resonant reactions**: standard R-Matrix approach cannot be applied to extract the resonance parameters of the B(x,C)D reaction because x is virtual → Modified R-Matrix [e.g. La Cognata et al. 2010] is introduced instead, where the cross section takes the form

$$\frac{d^2\sigma}{dE_{xA}d\Omega_s} = \mathrm{NF}\sum_\tau (2J_\tau + 1)$$

$$\times \left| \sqrt{\frac{k_f(E_{xA})}{\mu_{cC}}} \frac{\sqrt{2P_{l_\tau}(k_{cC}R_{cC})}M_\tau(p_{xA}R_{xA})\gamma_{cC\,\tau}\gamma_{xA\,\tau}}{D_\tau(E_{xA})} \right|^2$$

where:
- $M_\tau(p_{xa}R_{xa})$ describes the transfer amplitude for the QF-process (the transfer reaction, upper vertex)
- $\gamma_{xa\tau}$ and $\gamma_{Cc\tau}$ represents the reduced partial widths for the resonant excited states *that are the same of the direct measurements* → you can extract the γ's reduced widths from the THM reaction yield.

# TH measurements

| | Indirect reaction | Direct reaction | References |
|---|---|---|---|
| [1] | $^2$H$(^7$Li$,\alpha\alpha)$n | $^1$H$(^7$Li$,\alpha)^4$He | Spitaleri et al 1999, Lattuada et al 2001 [193] |
| [2] | $^3$He$(^7$Li$,\alpha\alpha)$d | $^2$H$(^7$Li$,\alpha)^4$He | Tumino et al 2006 [194] |
| [3] | $^2$H$(^6$Li$,\alpha^3$He$)$n | $^1$H$(^6$Li$,\alpha)^3$He | Tumino 2003 [84] |
| [4] | $^6$Li$(^6$Li$,\alpha\alpha)^4$He | $^2$H$(^6$Li$,\alpha)^4$He | Spitaleri et al 2001 [18] |
| [5] | $^2$H$(^9$Be$,\alpha^6$Li$)$n | $^1$H$(^9$Be$,\alpha)^6$Li | Wen et al 2008 [195] |
| [6] | $^2$H$(^{10}$B$,\alpha^7$Be$)$n | $^1$H$(^{10}$B$,\alpha)^7$Be | Lamia et al 2008, Rapisarda et al 2018, Cvetinovic et al 2018 [196, 197, 198] |
| [7] | $^2$H$(^{11}$B$,\alpha_0{}^8$Be$)$n | $^1$H$(^{11}$B$,\alpha)^8$Be | Spitaleri et al 2004, Lamia et al 2011 [199, 200] |
| [8] | $^2$H$(^{15}$N$,\alpha^{12}$C$)$n | $^1$H$(^{15}$N$,\alpha)^{12}$C | La Cognata et al 2007 [201] |
| [9] | $^2$H$(^{18}$O$,\alpha^{15}$N$)$n | $^1$H$(^{18}$O$,\alpha)^{15}$N | La Cognata et al 2009 [202] |
| [10] | $^2$H$(^{17}$O$,\alpha^{14}$N$)$n | $^1$H$(^{17}$O$,\alpha)^{14}$N | Sergi et al 2010, Sergi et al. 2015 [85, 86] |
| [11] | $^6$Li$(^3$He$,$p$^4$He$)^4$He | $^2$H$(^3$He$,$p$)^4$He | La Cognata et al 2005 [203] |
| [12] | $^2$H$(^6$Li$,$p$^3$H$)^4$He | $^2$H$($d$,$p$)^3$H | Rinollo et al 2005 [204] |
| [13] | $^6$Li$(^{12}$C$,\alpha^{12}$C$)^2$H | $^4$He$(^{12}$C$,^{12}$C$)^4$He | Spitaleri et al 2000 [205] |
| [14] | $^2$H$(^6$Li$,$t$^4$He$)^1$H | n$(^6$Li$,$t$)^4$He | Tumino et al 2005, Gulino et al 2010 [206, 207] |
| [15] | $^2$H$($p$,$pp$)$n | $^1$H$($p$,$p$)^1$H | Tumino et al 2007, Tumino et al 2008 [208, 209] |
| [16] | $^2$H$(^3$He$,$p$^3$H$)^1$H | $^2$H$(^2$H$,$p$)^3$H | Tumino et al 2011, Tumino et al 2014 [94, 89] |
| [17] | $^2$H$(^3$He$,$n$^3$He$)^1$H | $^2$H$(^2$H$,$n$)^3$He | Tumino et al 2011, Tumino et al 2014 [94, 89] |
| [18] | $^2$H$(^{19}$F$,\alpha^{16}$O$)$n | $^1$H$(^{19}$F$,\alpha)^{16}$O | La Cognata et al 2011, Indelicato et al 2017 [28, 139] |
| [19] | $^{13}$C$(^6$Li$,$n$^{16}$O$)^2$H | $^{13}$C$(\alpha,$n$)^{16}$O | La Cognata et al 2014 [210] |
| [20] | $^2$H$(^{18}$F$,\alpha^{15}$O$)$n | $^1$H$(^{18}$F$,\alpha)^{15}$O | Cherubini et al 2015, Pizzone et al. 2016, La Cognata et al., 2017 [211, 212, 213] |
| [21] | $^2$H$(^{10}$B$,\alpha^7$Li$)^1$H | n$(^{10}$B$,\alpha)^7$Li | Guardo et al 2019, Sparta et al 2021 [214, 215] |
| [22] | $^2$H$(^7$Be$,\alpha\alpha)^1$H | n$(^7$Be$,\alpha)^4$He | Lamia et al 2017, Lamia et al 2019, Hayakawa et al 2021 [106, 108, 110] |
| [23] | $^{12}$C$(^{14}$N$,\alpha^{20}$Ne$)^2$H | $^{12}$C$(^{12}$C$,\alpha)^{20}$Ne | Tumino et al 2018 [26] |
| [24] | $^{12}$C$(^{14}$N$,$p$^{23}$Na$)^2$H | $^{12}$C$(^{12}$C$,$p$)^{23}$Na | Tumino et al 2018 [26] |
| [25] | $^6$Li$(^{19}$F$,p^{22}$Ne$)^2$H | $^4$He$(^{19}$F$,$p$)^{22}$Ne | Pizzone et al 2017, Dagata et al 2018 [212, 216] |
| [26] | $^2$H$(^{17}$O$,\alpha^{14}$C$)^1$H | $^{17}$O$($n$,\alpha)^{14}$C | Oliva et al 2020 [217] |
| [27] | $^2$H$(^3$He$,pt)^1$H | $^3$He$($n$,$p$)^3$H | Pizzone et al 2021 [218] |
| [28] | $^2$H$(^7$Be$,$p$^7$Li$)^1$H | n$(^7$Be$,$p$)^7$Li | Hayakawa et al 2021 [110] |
| [29] | $^2$H$(^{27}$Al$,\alpha^{24}$Mg$)$n | $^{27}$Al$($p$,\alpha)^{24}$Mg | Palmerini et al 2021, La Cognata et al. 2022 [137, 135, 136] |

*[Tumino et al., 2025,*
*Progress on Particle and Nuclear Physics]*

About the He-burning

$3\alpha \rightarrow {}^{12}$C, $^{12}$C$(\alpha,\gamma)^{16}$O etc.
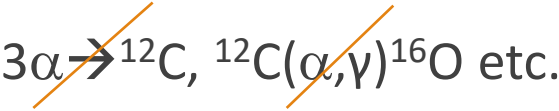
«Other» (not about energy prod.) reactions:
- $^{18}$O$($p$,\alpha)^{15}$N & $^{14}$N$($n,p$)^{14}$C $\rightarrow$ fluorine nucleosynthesis
- $^{13}$C$(\alpha,$n$)^{16}$O & $^{22}$Ne$(\alpha,$n$)^{25}$Mg $\rightarrow$ s-process n supply

# $^{18}O(p,\alpha)^{15}N$

*(credits to M. La Cognata)*

# $^{18}O(p,\alpha)^{15}N$  *(credits to M. La Cognata)*

three-body process → $^2H(^{18}O,\alpha^{15}N)n$:
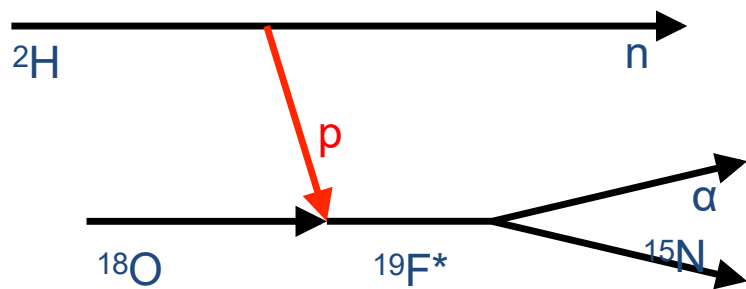
$E_b$=54MeV, CD$_2$ target 100 µg/cm$^2$
telescope A for $^{15}N$ detection
3 PSDs (B, C, D) (no ∆E, to lower
detection thresholds)



²H                    n

p

α
¹⁸O        ¹⁹F*    ¹⁵N
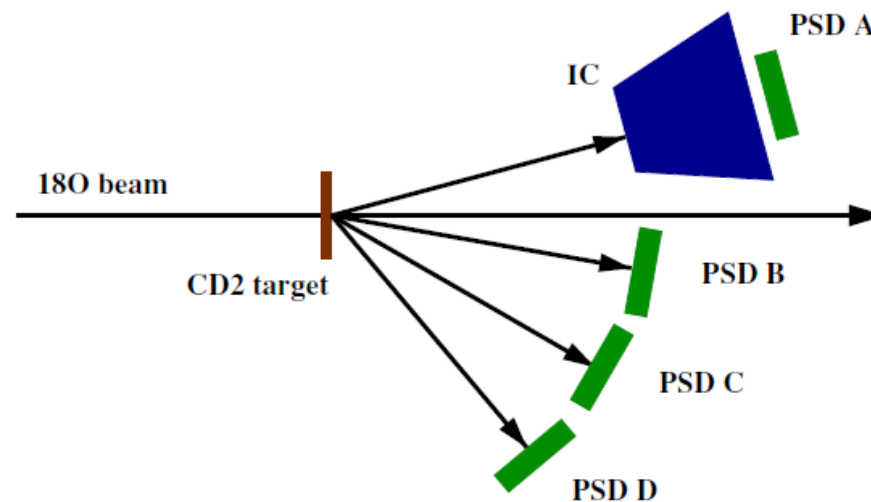
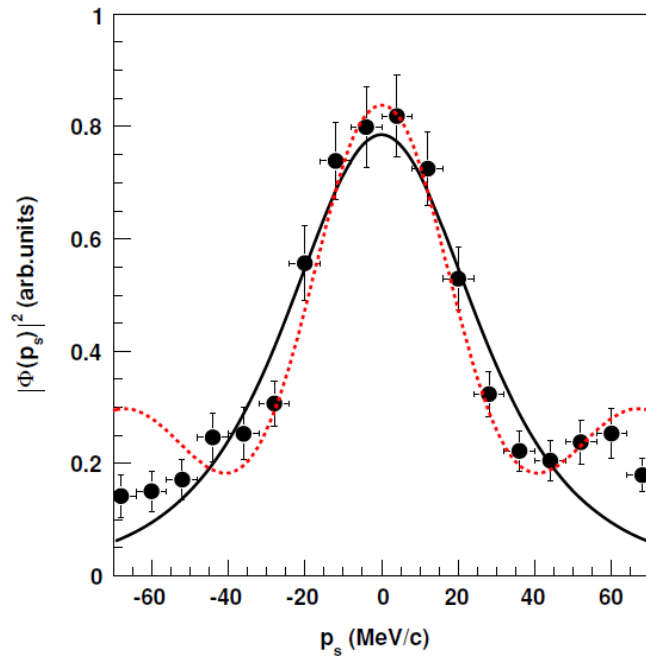[La Cognata+,PRL2008]
[La Cognata+,ApJ2010 vol708 «A novel approach…»]
[La Cognata+,ApJ2010 vol723 «Effect of high-energy resonances…»]



IC                    PSD A

18O beam

CD2 target            PSD B

PSD C

PSD D

# $^{18}O(p,\alpha)^{15}N$

# $^{18}O(p,\alpha)^{15}N$
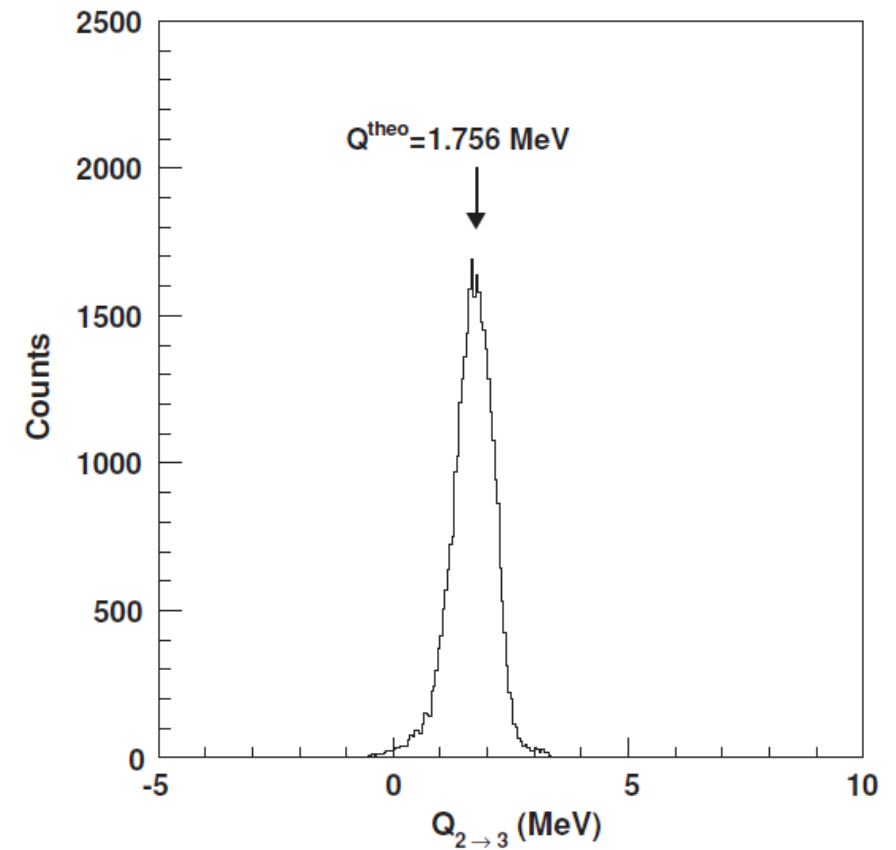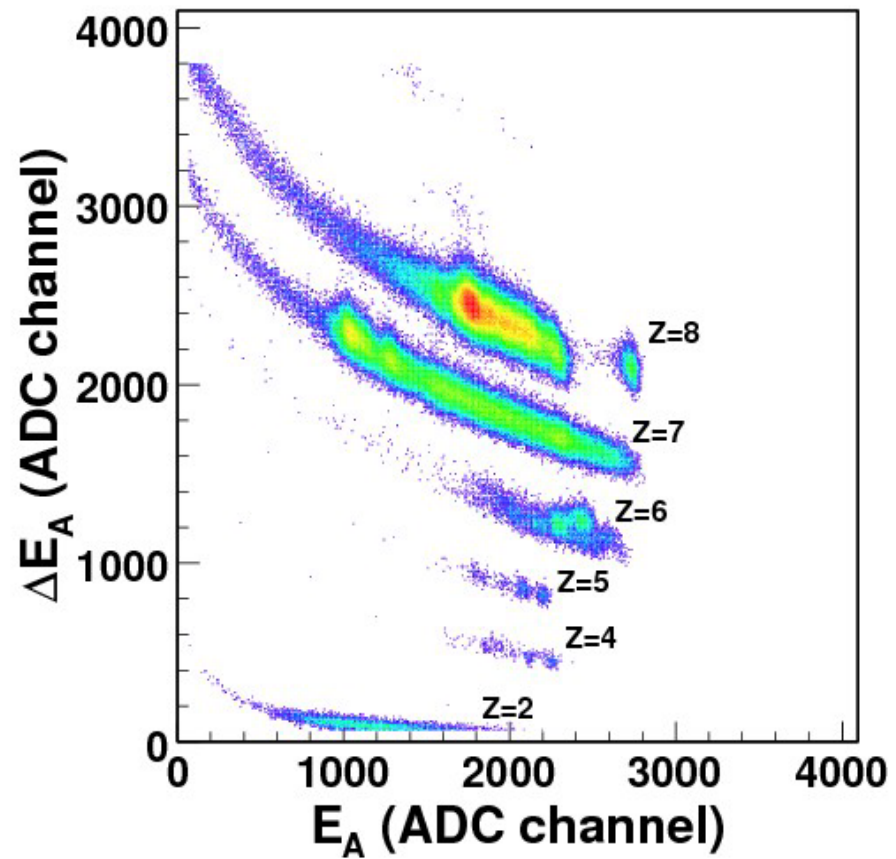


**DWBA momentum distribution
(potential parameters from Perey & Perey)
Distortions negligible below 50 MeV/c**

**Good agreement inside a 50 MeV/ c momentum window**

*«Distortions, if any, should influence only the tails of the distribution (Spitaleri et al. 2004), beyond the range of interest, corresponding to short n-p relative distances, as only the nuclear interaction can influence the $^{18}O$-p interaction.»*

# $^{18}O(p,\alpha)^{15}N$



**~50 resonances in the 0-7 MeV region**, but the main contribution to RR is given by the resonances:

1. **20 keV** $J^\pi=5/2^+$
2. **144 keV** $J^\pi=1/2^+$ (well established)
3. **656 keV** $J^\pi=1/2^+$

The 656 keV resonance provides a significant contribution to the reaction rate both at low and high temperatures. The strength and FWHM of the 656 keV are very uncertain **(~ 300%).**
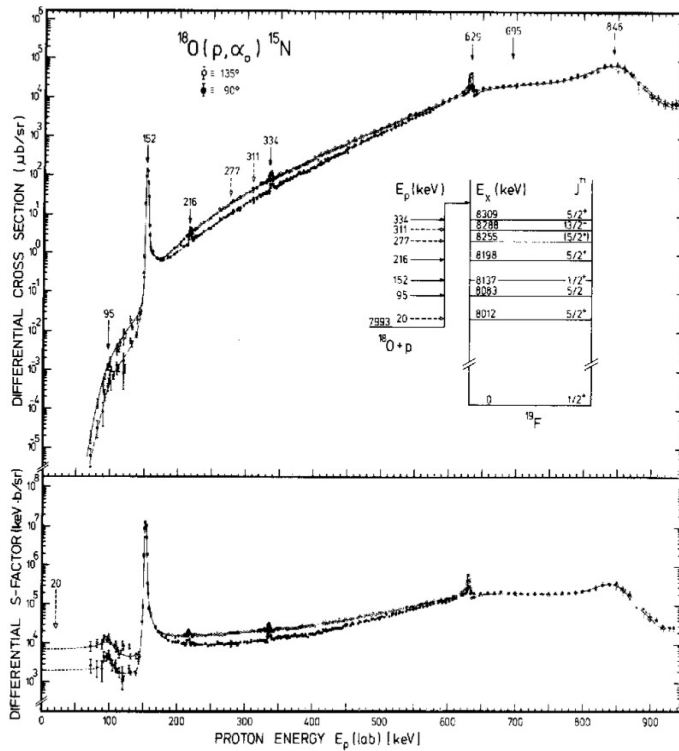
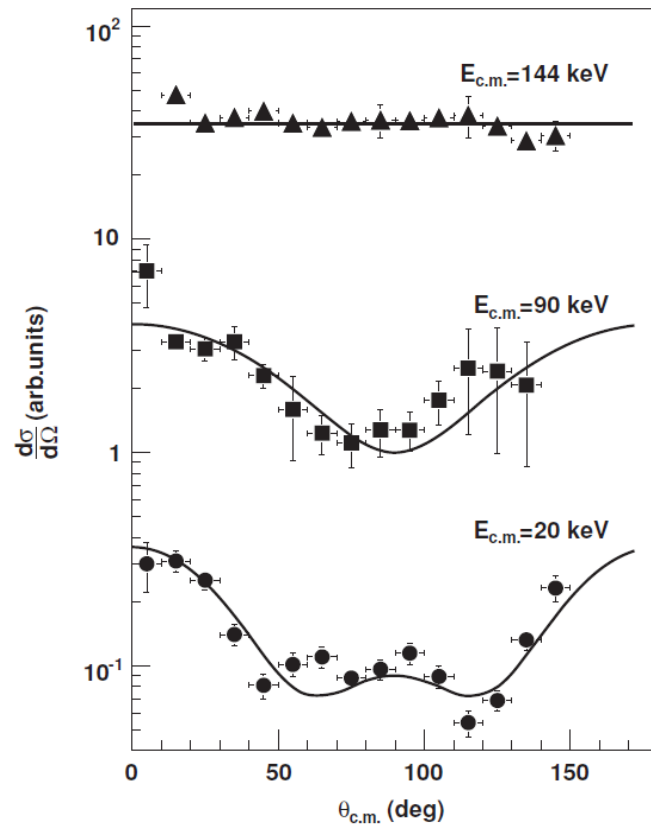> *Modified R-Matrix is introduced*

In the case of a <span style="color:red">resonant</span> THM reaction the cross section takes the form

$$\frac{d^2\sigma}{dE_{Cc}\,d\Omega_s} \propto \frac{\Gamma_{(Cc)_i}(E)\,|M_i(E)|^2}{(E - E_{R_i})^2 + \Gamma_i^2(E)/4}$$

**$M_i(E)$** is the amplitude of the transfer reaction (upper vertex) that can be easily **calculated**

→ The resonance parameters can be extracted and in particular the strength

# $^{18}O(p,\alpha)^{15}N$



Assignment of spin and parity of the resonances is obtained by fitting     the angular distribution with the formula

$$\frac{d\sigma}{d\Omega_{c.m.}} = \frac{d\sigma}{d\Omega_{c.m.}}(90°)\left(1 + A_2(E)\cos^2\theta \right.$$
$$\left. + A_4(E)\cos^4\theta + ... + A_{2L}(E)\cos^{2L}\theta\right)$$

144 keV → 1/2⁺ (isotropic angular distributions, L=0)
90 keV → 3/2⁺ (L=1)
20 keV → 5/2⁺ (L=2)
20  keV  and  144 keV assignments in agreement with literature
90 keV → first time assignment

# $^{18}O(p,\alpha)^{15}N$ (Extracting resonance strength)

*Narrow resonances dominating S-factor → reaction rate can be calculated by means of the resonance strength*

$$(\omega\gamma)_i = \frac{\hat{J}_i}{\hat{J}_p \hat{J}_{18_O}} \frac{\Gamma_{(p^{18}O)_i}(E_{R_i})\, \Gamma_{(\alpha^{15}N)_i}(E_{R_i})}{\Gamma_i(E_{R_i})}$$

Where:
- $\hat{J}=2J+1$
- $\Gamma_{(AB)}$ is the partial width for the A+B channel
- $\Gamma_i$ is the total with of the i-th resonance
- $E_{R_i}$ is the resonance energy

In the THM approach:

$$(\omega\gamma)_i = \frac{1}{2\pi}\omega_i N_i \frac{\Gamma_{(p^{18}O)_i}}{|M_i|^2}$$
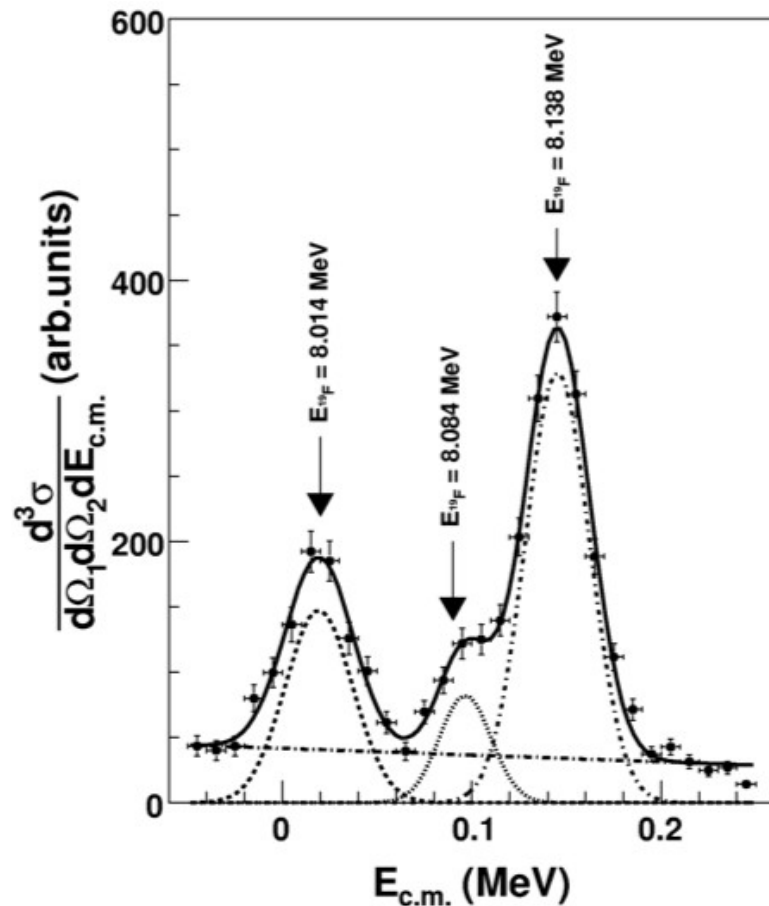
Where:
- $\omega_I = \hat{J}_i / \hat{J}_p \hat{J}_{18_O}$ statistical factor
- $N_i$ = THM resonance strength
- $M_i$ = transfer amplitude

<span style="color:red">Advantages:</span>
- possibility to measure down to zero energy
- No electron screening
- No spectroscopic factors in the $\Gamma_{(p18O)} / |M_i|^2$ ratio

# $^{18}$O(p,$\alpha$)$^{15}$N (Extracting resonance strength)
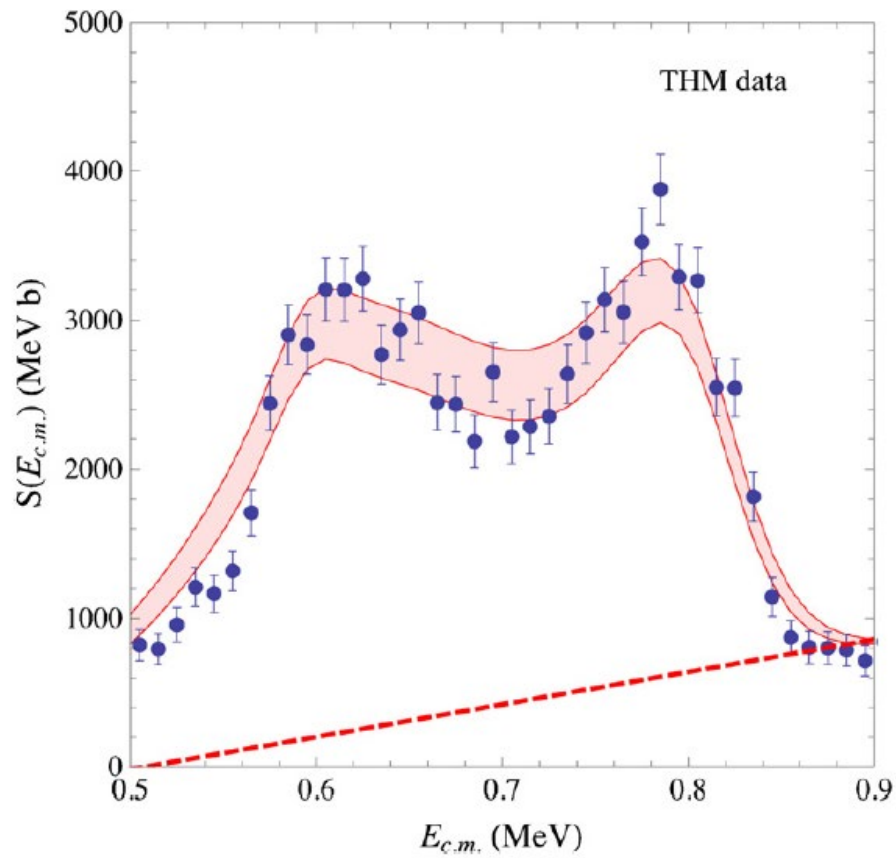


Present case: narrow resonances.

THM data are smoothed out because of 17 keV energy spread

**Absolute values are obtained by normalizing to the well known resonance at 144 keV**

$$(\omega\gamma)_i = \frac{\omega_i}{\omega_3} \frac{\Gamma_{p_i}(E_{R_i})}{|M_i(E_{R_i})|^2} \frac{|M_3(E_{R_3})|^2}{\Gamma_{p_3}(E_{R_3})} \frac{N_i}{N_3} (\omega\gamma)_3$$

| $\omega\gamma$ (eV) | Present work | NACRE |
|---|---|---|
| 20 keV | $(8.3\,^{+3.8}_{-2.6})*10^{-19}$ | $(6\,^{+17}_{-5}) * 10^{-19}$ |
| 90 keV | $(1.8 \pm 0.3)*10^{-7}$ | $(1.6 \pm 0.5)*10^{-7}$ |

# $^{18}O(p,\alpha)^{15}N$



Modified *R*-matrix fitting (red band) of the THM *S(E)* factor (blue points).
The fitting parameters have been determined by simultaneously fitting the Lorentz-Wirzba et al. (1979) and THM data (present work)
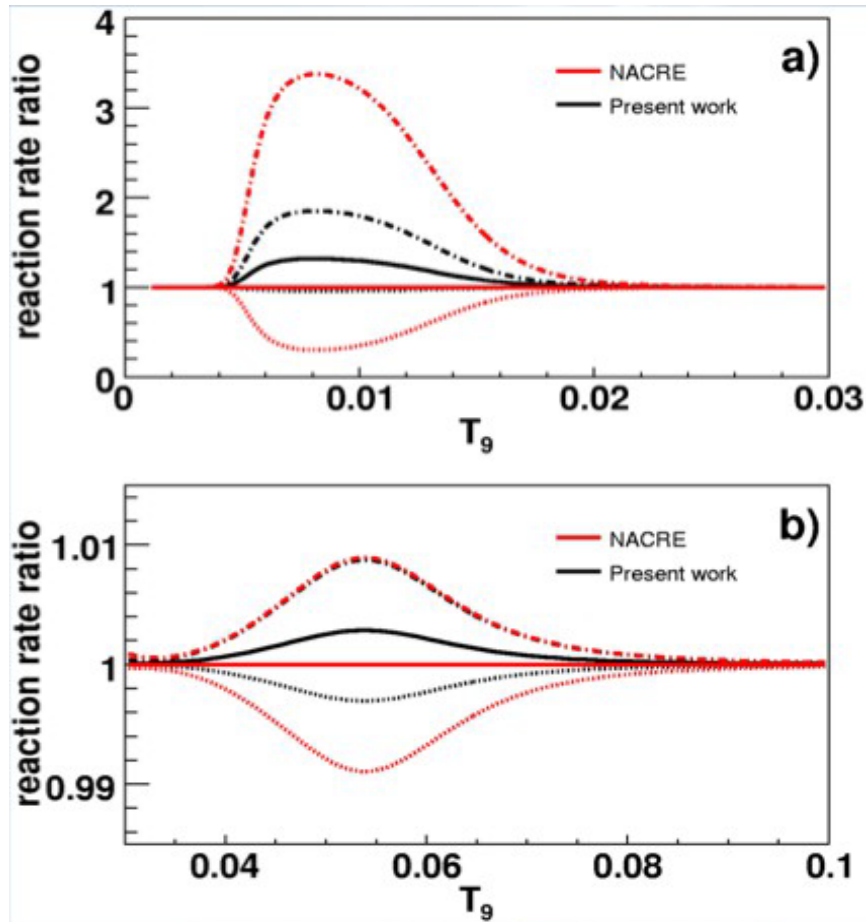
(energy resolution taken into account by convoluting the fit with the 17 keV energy resolution)

660 keV and 799 keV Resonance Parameters from the Simultaneous Fitting of Lorentz-Wirzba et al. (1979) and THM data

|   | $E_R$ (keV) | $\Gamma_p$ (keV) | $\Gamma_\alpha$ (keV) | $\Gamma_{tot}$ (keV) |
|---|---|---|---|---|
| 1 | $609 \pm 2$ | $11.1 \pm 1.1$ | $188 \pm 3$ | $199 \pm 3$ |
| 2 | $812.5 \pm 1.5$ | $27 \pm 10$ | $40^{+5}_{-13}$ | $67^{+11}_{-16}$ |

**$E_R$ ~ 50 keV smaller than literature**
**Width error 50% → 1.5%**

# $^{18}O(p,\alpha)^{15}N$
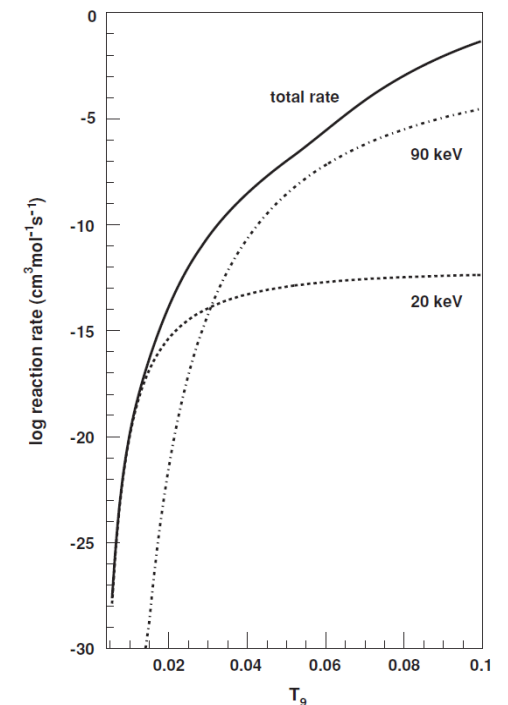


The contribution to the reaction rate of each resonance is given by:

$$N_A \langle \sigma v \rangle_R = 1.5394 \times 10^{11} A^{-3/2} (\omega\gamma) T_9^{-3/2} \exp(-11.605 E_r / T_9)$$

If T9 < 0.03 (fig a) the RR can be about 35% larger than the one given by NACRE, while indetermination  is greatly  reduced  (a factor 8.5)
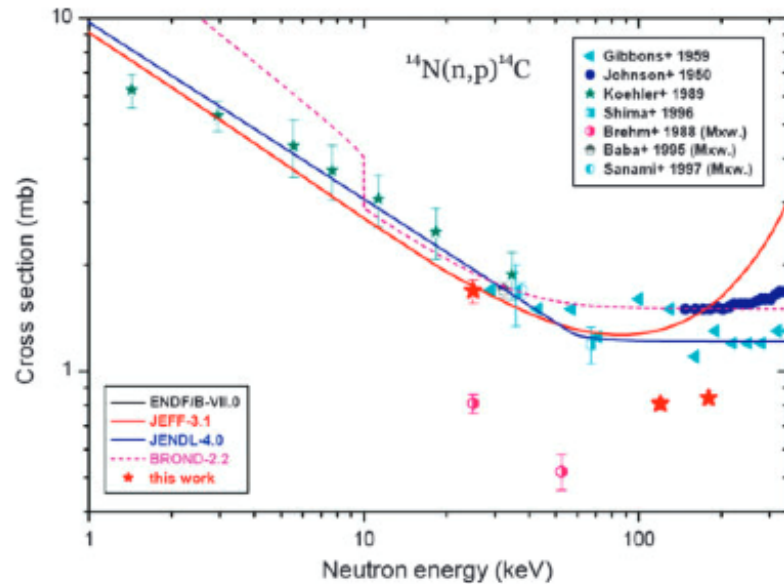
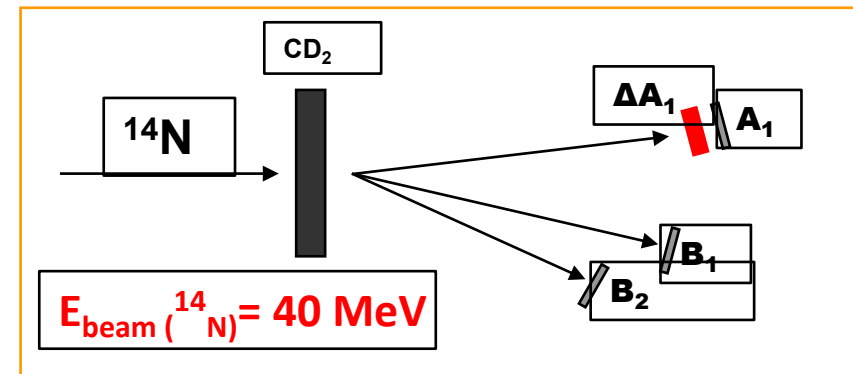# $^{14}N(n,p)^{14}C$
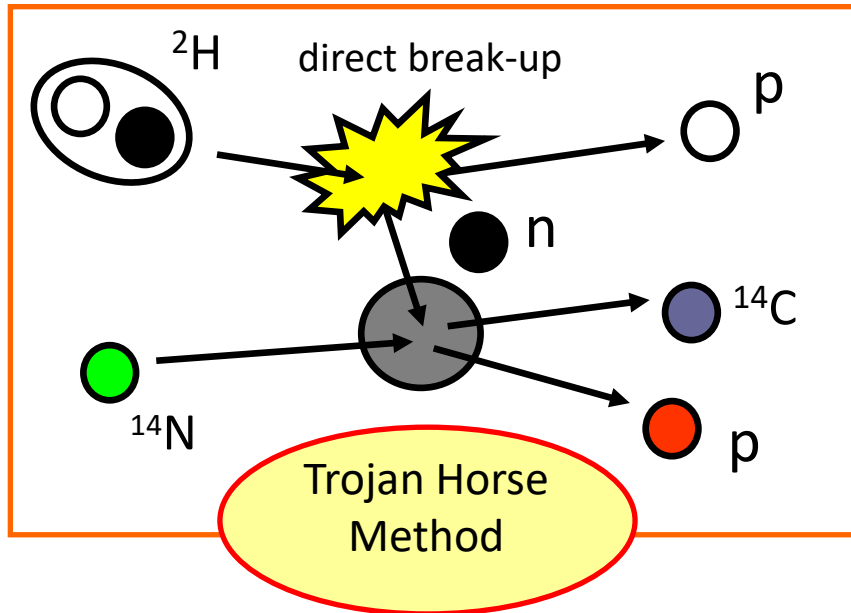
*(credits to M.L. Sergi)*

# $^{14}N(n,p)^{14}C$

*(credits to M.L. Sergi)*
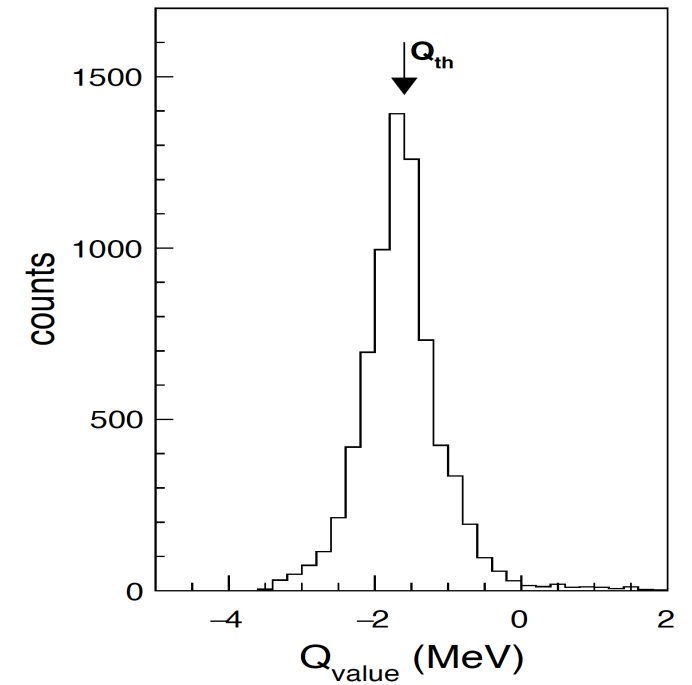
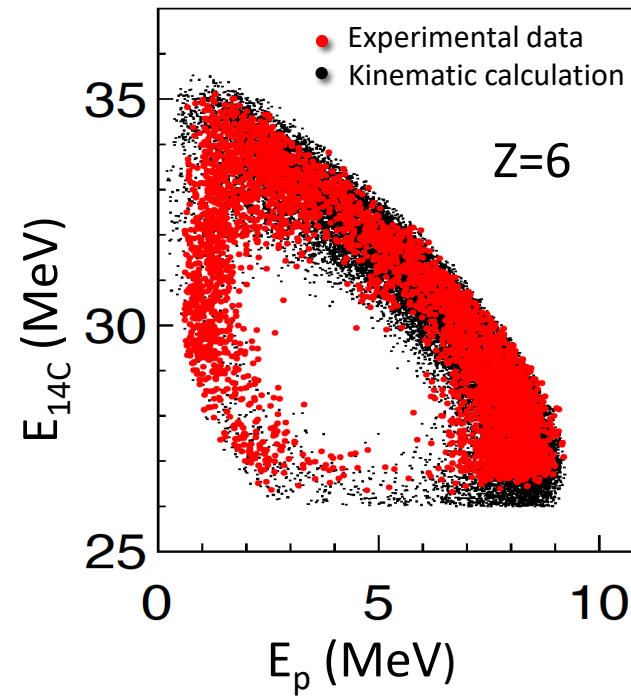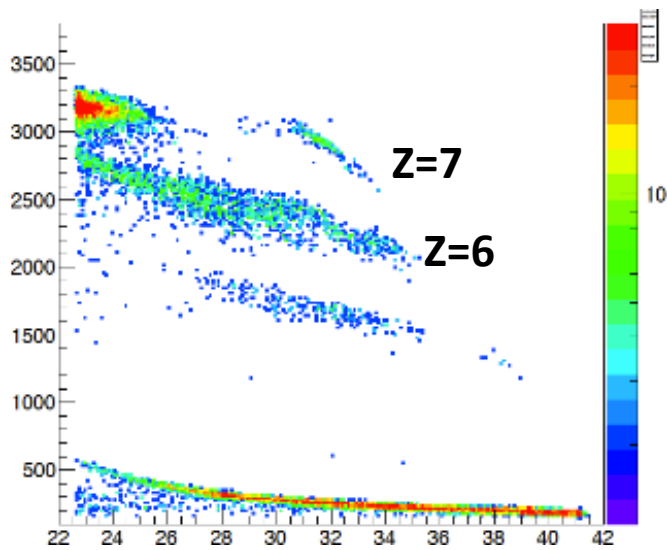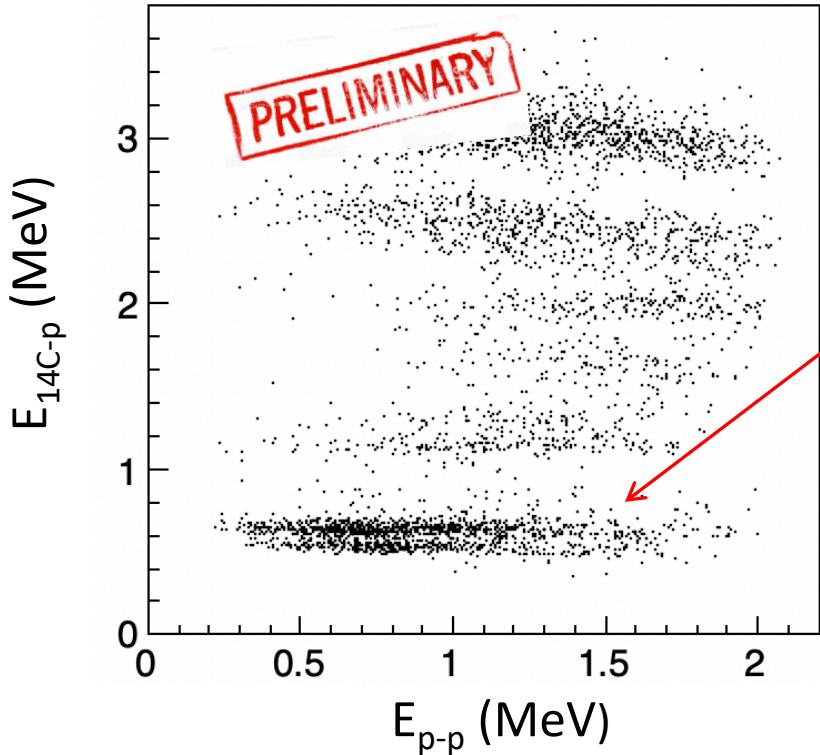Wallner et al., Astronomical Society of Australia, (2012), 29, 115



He-burning shell in AGBs: primary site for F synthesis
$^{14}N(\alpha,\gamma)^{18}F(\beta^+)^{18}O(p,\alpha)^{15}N(\alpha,\gamma)^{19}F$

$\rightarrow$ protons captured by $^{18}O$ are mostly coming from $^{14}N(n,p)^{14}C$ reaction

# $^{14}N(n,p)^{14}C$



direct break-up

Trojan Horse Method



$E_{beam\,(^{14}N)} = 40\ MeV$

| Detectors | Thickness [μm] | θ [deg] | r [cm] | Δθ [deg] |
|---|---|---|---|---|
| $A_1$ (STRIP) | 500 | 5.0 ± 0.1 | 80 | ±1.8 |
| $\Delta A_1$ (STRIP) | 20 | 5.0 ± 0.1 | 80 | ±1.8 |
| $B_1$ (STRIP) | 1000 | 25.0 ± 0.1 | 25 | ±5.7 |
| $B_2$ (PSD) | 500 | 40.0 ± 0.1 | 25 | ±5.7 |

# $^{14}$N(n,p)$^{14}$C

# $^{14}N(n,p)^{14}C$



$E_{p\text{-}p}$ (MeV)

$E_{14C\text{-}p}$ (MeV)

subthreshold levels

The clear horizontal loci in $E_{14C\text{-}p}$ represent an evidence for the formation of the $^{15}N$ excited states.

**$E_{15N^*}$ (MeV)**

| $E_{14C\text{-}p}$ (MeV) | $E_x$ (MeV ± keV) | $J^\pi; T$ |
|---|---|---|
| | $9.9250 \pm 0.2$ | $\frac{3}{2}^-$ |
| | $10.0660 \pm 0.2$ [c] | $\frac{3}{2}^+$ |
| 0.411 MeV | $10.4497 \pm 0.3$ | $\frac{5}{2}^-$ |
| 0.495 MeV | $10.5333 \pm 0.5$ | $\frac{5}{2}^+$ |
| | $10.6932 \pm 0.3$ | $\frac{9}{2}^+$ |
| 0.553 MeV | $10.7019 \pm 0.3$ | $\frac{3}{2}^-$ |
| 0.655 MeV | $10.804 \pm 2$ | $\frac{3}{2}^+$ |
| 1.028 MeV | $11.235 \pm 5$ [b] | $\geq \frac{3}{2}$ |
| 1.086 MeV | $11.2928 \pm 0.7$ | $\frac{1}{2}^-$ |
| 1.231 MeV | $11.4376 \pm 0.7$ | $\frac{1}{2}^+$ |
| 1.408 MeV | $11.615 \pm 4$ | $\frac{1}{2}^+; T = \frac{3}{2}$ |
| 1.556 MeV | $11.763 \pm 3$ | $\frac{3}{2}^+$ |
| | $11.876 \pm 3$ | $\frac{3}{2}^-$ |
| | $11.942 \pm 6$ | $\frac{3}{2}^-$ |
| | $11.965 \pm 3$ | $\frac{1}{2}^-$ |
| . | $12.095 \pm 3$ | $\frac{5}{2}^+$ |
| | $12.145 \pm 3$ | $\frac{3}{2}^-$ |
| . | $12.327 \pm 4$ | $\frac{5}{2}^{(+)}$ |
| | $12.493 \pm 4$ | $\frac{5}{2}^+; \frac{1}{2}$ |
| . | $12.522 \pm 8$ | $\frac{5}{2}^+; \frac{1}{2}$ |
| | $12.551 \pm 10$ | $\frac{9}{2}^+$ |
| . | $12.920 \pm 4$ | $\frac{3}{2}^-$ |
| | $12.940 \pm 10$ | $\frac{5}{2}^+$ |
| . | $13.004 \pm 10$ | $\frac{11}{2}^-$ |
| | $13.149 \pm 10$ | |
| . | $13.174 \pm 7$ | $\left(\frac{9}{2}\right)$ |
| 3.155 MeV | $13.362 \pm 8$ | $\frac{3}{2}^-$ |
| | $13.390 \pm 10$ | $\frac{3}{2}^+$ |

# $^{14}N(n,p)^{14}C$



*Data analysis ongoing (near the end)*

# $^{13}C(\alpha,n)^{16}O$

*(credits to M. La Cognata)*

# $^{13}C(\alpha,n)^{16}O$

$^{13}C(^6Li,n^{16}O)d$



**EXPERIMENTAL SETUP**



**$^6Li$ beam (8 MeV) on $^{13}C$ target**
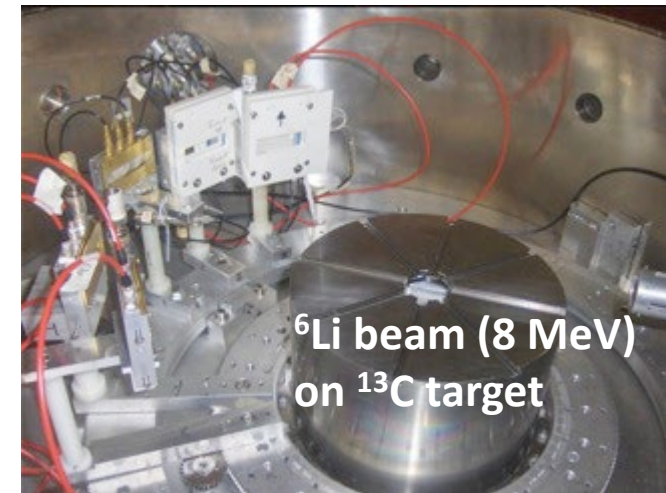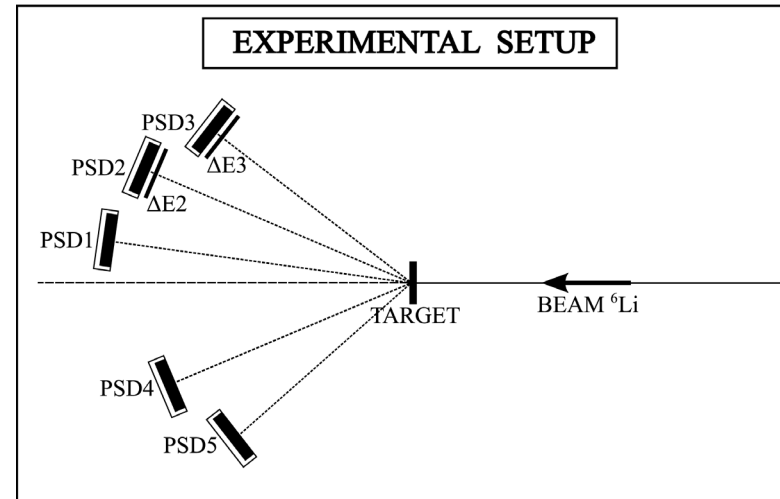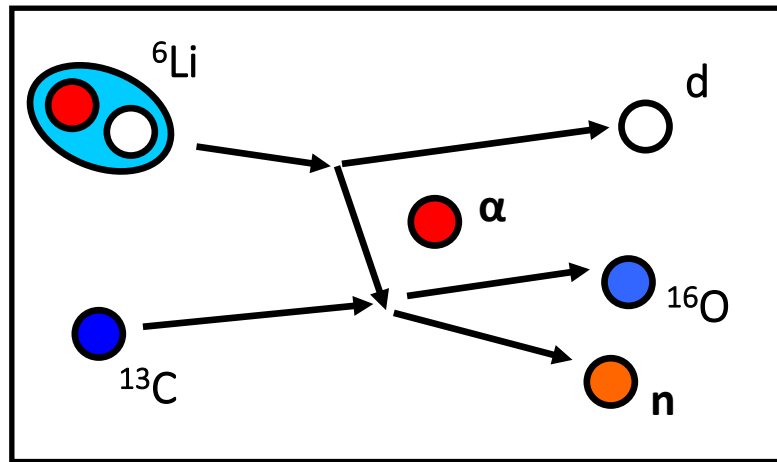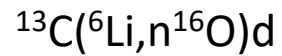
d detection in PSD 1-2-3 → No need for neutron detectors
d is emitted at 0° → QF peak cannot be accessed in the experiment

FLORIDA STATE UNIVERSITY
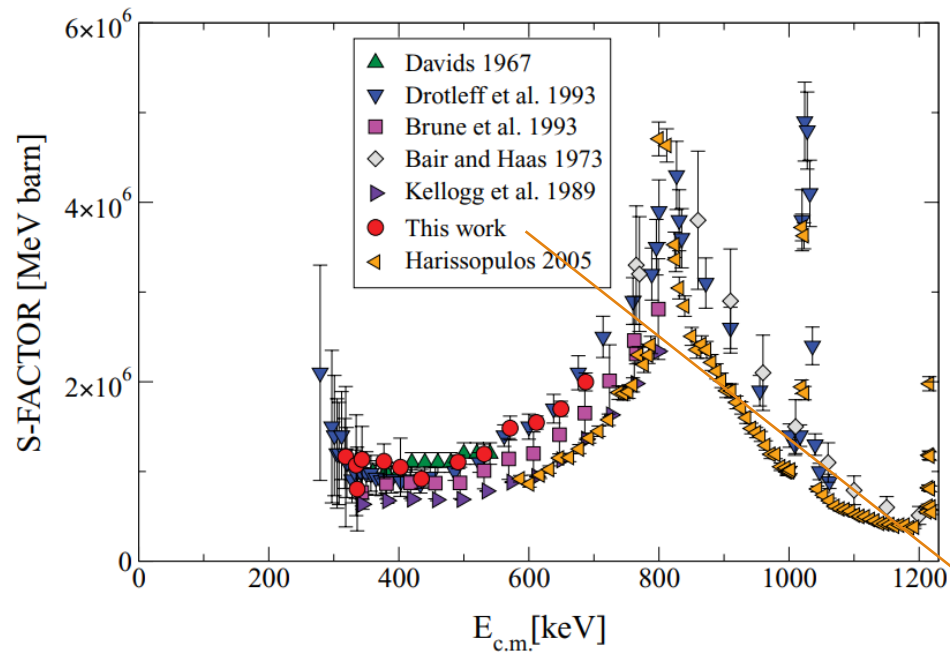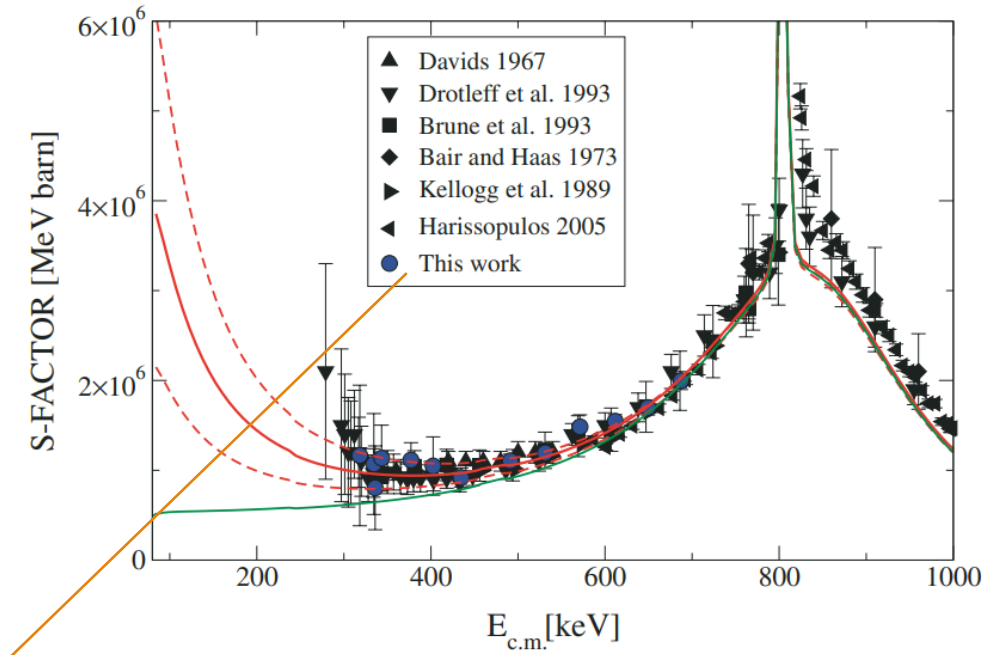
# $^{13}C(\alpha,n)^{16}O$

# Heil scaling

Direct Data from literature
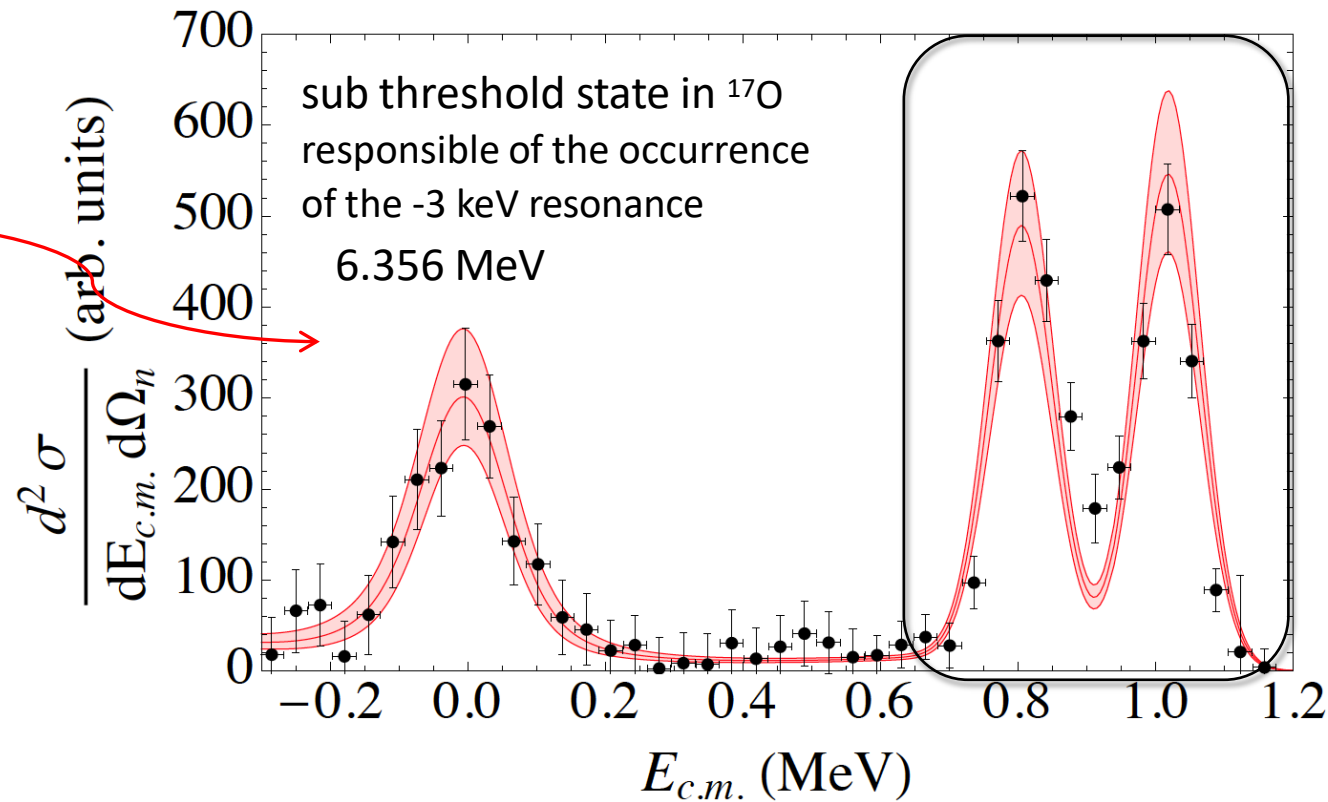
Direct Data scaled to the Heil data (global R-matrix fit)



[Heil+,PRC2008]

# $^{13}C(\alpha,n)^{16}O$ Normalization to "Heil scaled data"

Fitted HOES cross section:
2 parameters, the reduced n-
and $\alpha$- widths.
Channel radii fixed at the Heil
et al. ones [5.2 and 4 fm for
the $\alpha$- and n- channels]

sub threshold state in $^{17}O$
responsible of the occurrence
of the -3 keV resonance

6.356 MeV

Normalization region:
Scaling factor and energy
resolution obtained (this
one in agreement with the
calculated one, 46 keV)



**With this normlization TH data give ANC not in agreement with literature!**

# $^{13}C(\alpha,n)^{16}O$      ANC measurements

**Table 1**

Summary of Widths and ANC Values for the 1/2$^+$ State of $^{17}$O Close to the $^{13}$C $-$ $\alpha$ Threshold Reported in the Literature

| Reference | $\Gamma_n$ (keV) | ANC (fm$^{-1}$) |
|---|---|---|
| Fowler et al. (1973) | 124 | ... |
| Tilley et al. (1993) | 124 $\pm$ 12 | ... |
| Sayer (2000) | 162.37 | ... |
| Johnson et al. (2006) | 124 $\pm$ 12 | 0.89 $\pm$ 0.23 |
| Pellegriti et al. (2008) | 124 $\pm$ 8 | 4.5 $\pm$ 2.2 |
| Heil et al. (2008) | 158.1 | ... |
| La Cognata et al. (2012) | $83^{+9}_{-12}$ | $6.7^{+0.9}_{-0.6}$ |
| Guo et al. (2012) | 124 | 4.0 $\pm$ 1.1 |
| La Cognata et al. (2013) | $107 \pm 5_{stat}{}^{+9}_{-5\,norm}$ | $7.7 \pm 0.3_{stat}{}^{+1.6}_{-1.5\,norm}$ |
| Faestermann et al. (2015)$^a$ | 136 $\pm$ 5 | ... |
| Avila et al. (2015) | ... | 3.6 $\pm$ 0.7 |

*FINDING THE CONCORDANCE SCENARIO*

The ANC for the 6.356 MeV state is deduced from the fitting of the angular distribution of the sub-Coulomb alpha transfer off $^6$Li to $^{13}$C.

Agreement for ANC and not for S(E) → instead of normalize to the 2 resonances at higher energies, we normalize to the ANC of the 4.7 keV resonance (ex -3 keV res.), $\Gamma_n$=136±5 keV in Faestermann et al. (2015),

ANC value (observable) of 3.6±0.7 fm$^{-1}$ of Avila et al. (2015)

Using these values for the 1$^{st}$ resonance, we see what happens to the other two resonances in the many data sets.

*ANC-resonances parameters (bound and unbound states) in [Mukhamedzhanov&Tribble,PRC1999]*

# $^{13}C(\alpha,n)^{16}O$

TO SINGLE OUT THE "CORRECT DATA SETS TO NORMALIZE TO"

(a) blue (Davids 1968), orange (Drotleff et al. 1993), and pink (Heil et al. 2008) symbols;
(b) black (Bair & Haas 1973) and orange (Drotleff et al. 1993) for the low-energy region ($Ec.m. < 0.75$ MeV);
(c) c) purple (Kellogg et al. 1989) and green (Harissopulos et al. 2005)

*Left panel: direct data sets when fixing ANC of the 1° res. to Avila et al. (2015) with corresponding R-matrix*
*Right panels: HOES R-matrix fit of the THM data presented in La Cognata et al. (2013) (solid black symbols) adopting **the same resonance parameters** used in the corresponding left panel (color of the curves is the same for OES-HOES calculation).*

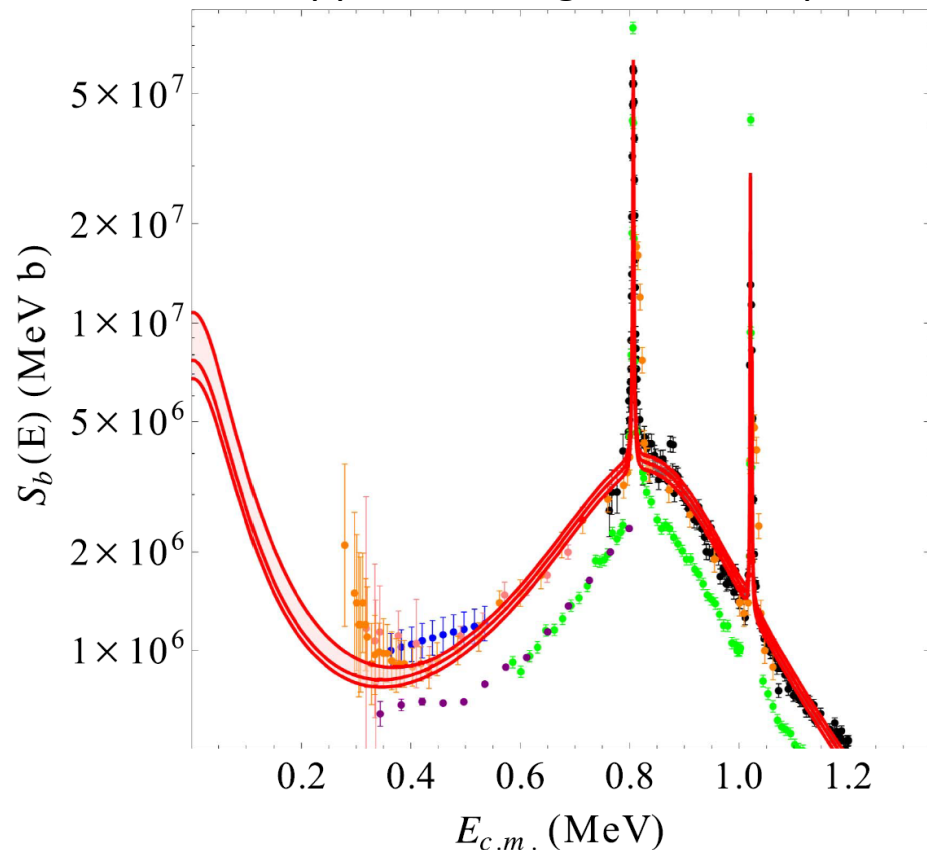→Best $\chi^2$ for THM normalization: panels (b) and (e)
This means that (b) direct data sets are consistent with ANC weighted mean and so are good for TH normalization.



[Trippella&LaCognata2017,ApJ]
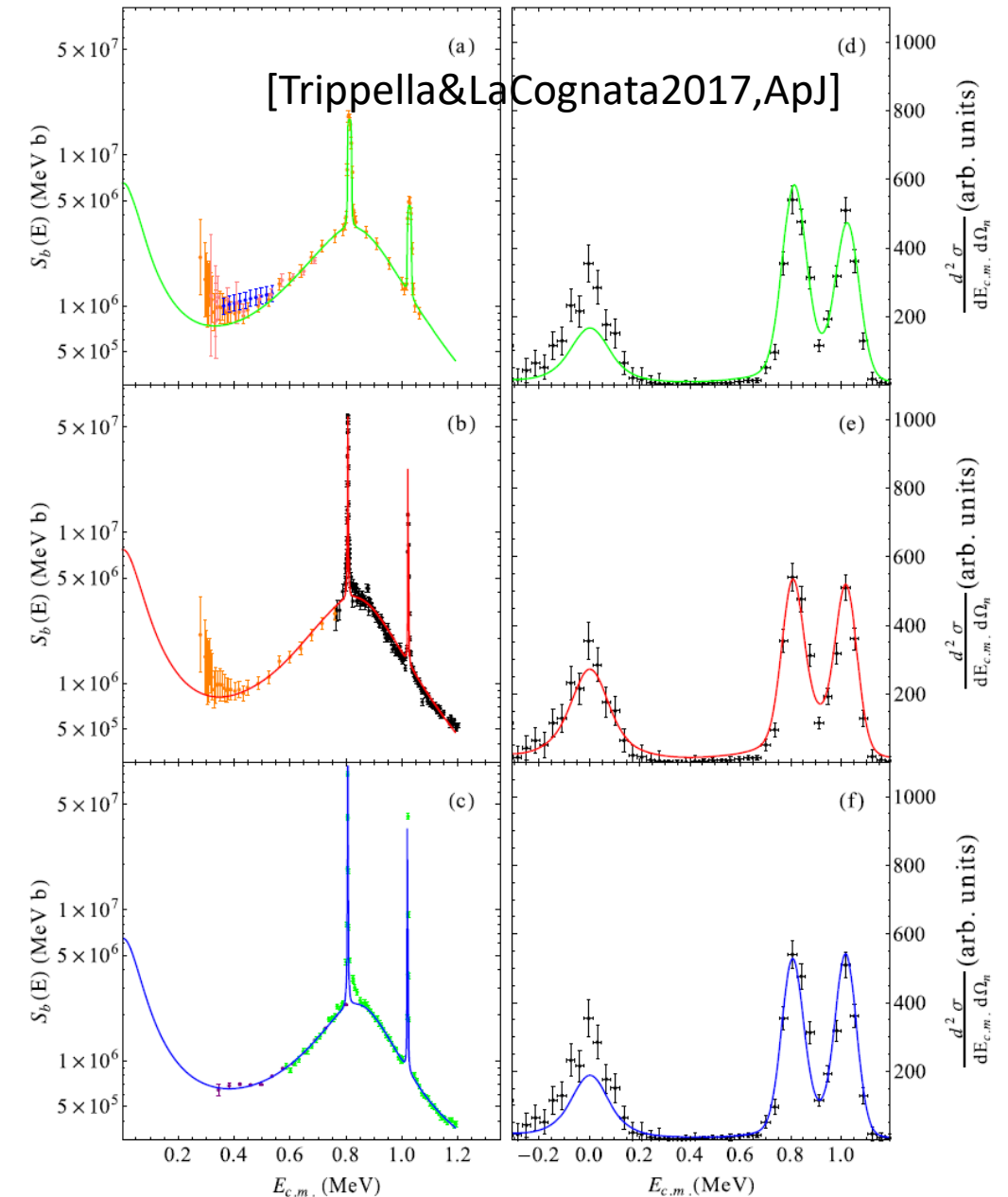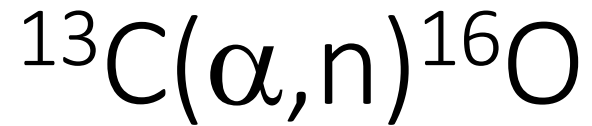
# $^{13}C(\alpha,n)^{16}O$

# The results

[Trippella&LaCognata2017,ApJ]



R-matrix astrophysical factor (central red curve) calculated adopting the resonance parameters used in panels (b) and (e).
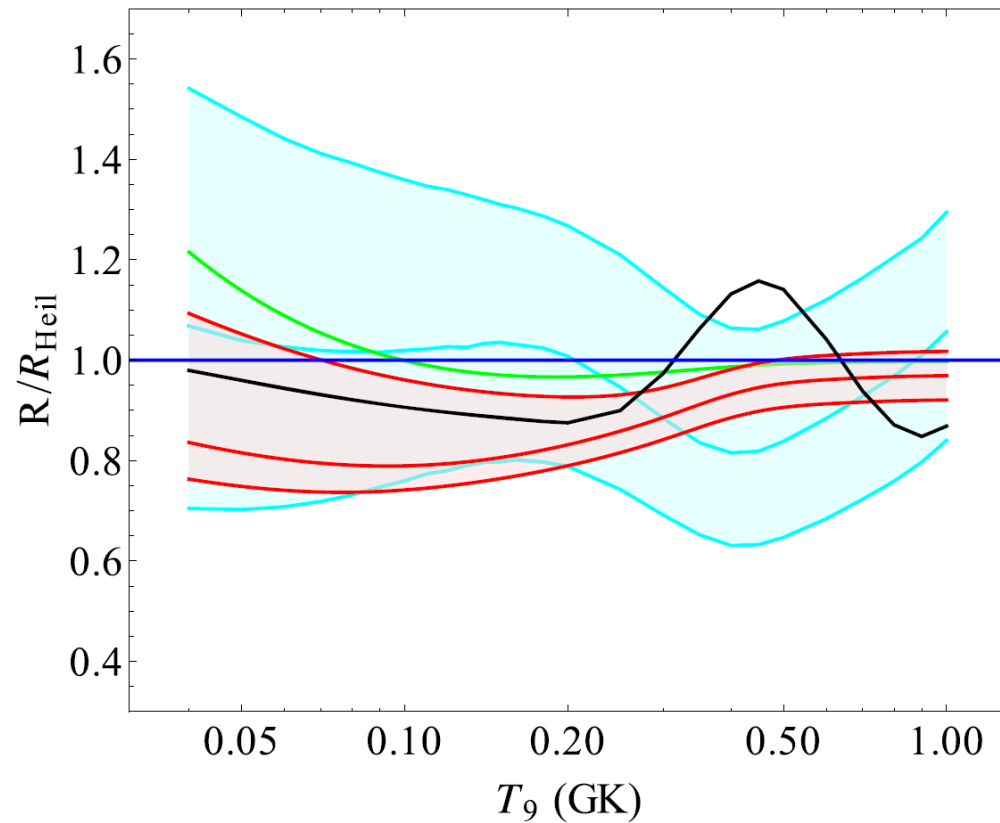
Direct data (without assuming any normalization):
Davids (1968)                      blue
Bair & Haas (1973)              black
Kellogg et al. (1989)           purple
Drotleff et al. (1993)           orange
Harissopulos et al. (2005)   green
Heil et al. (2008)                 pink

# $^{13}C(\alpha,n)^{16}O$

# The results

[Trippella&LaCognata2017,ApJ]



| | |
|---|---|
| Red band | RR by Trippella&LaCognata 2017 |
| Green curve | RR by La Cognata et al. (2013) |
| Black curve | RR by Drotleff et al. (1993) |
| Cyan band | NACRE II (Xu et al. 2013) |

# $^{13}C(\alpha,n)^{16}O$-Comparison with DeBoer+2020

Unfortunately, comparison is carried out with the outdated La Cognata et al 2013 results

If the comparison is done with Trippella & La Cognata 2017, good agreement is found (which is to be expected as the ANC from Avila et al is consided in the R-matrix analysis)

# $^{13}C(\alpha,n)^{16}O$-Comparison with Ciani+ 2021
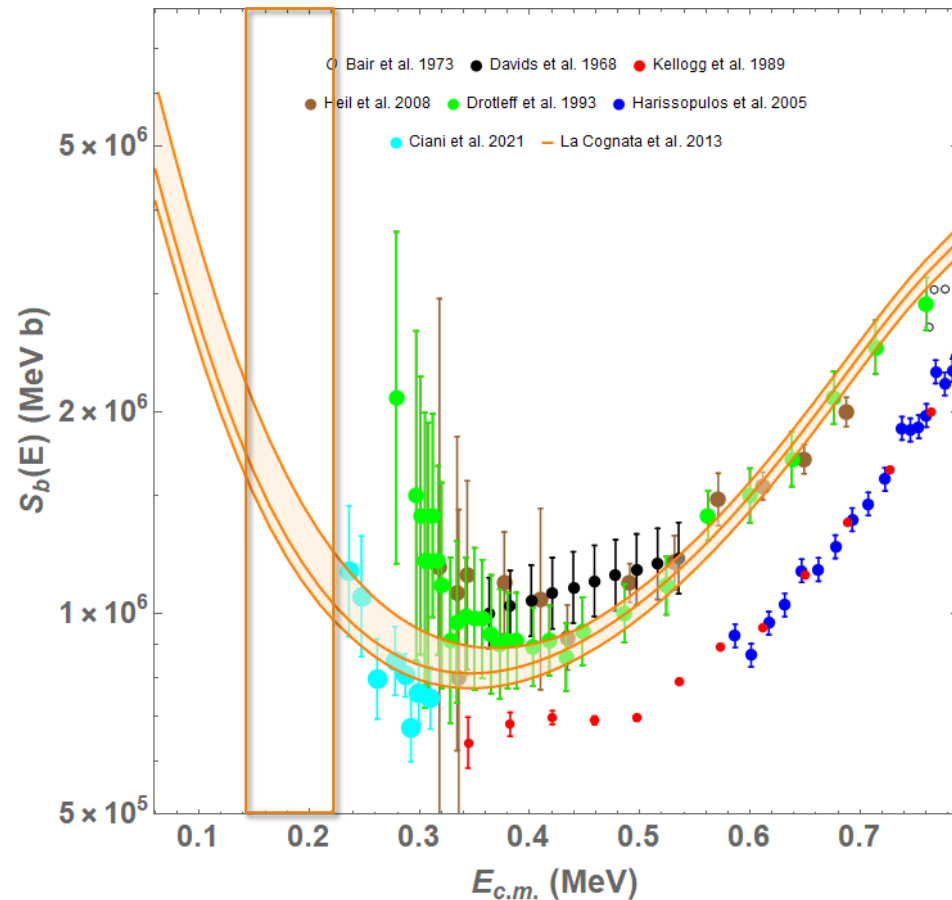


**ORANGE:** THM [Trippella&LaCognata2017,ApJ]

**CYAN:** experimental data measured underground LUNA Collaboration [Ciani+,PRL2021]

highlighted box = Gamow window = 150-230 keV

*The high accuracy direct measurement by Ciani et al. (2021) confirms the THM+ANC results obtained in 2017 → towards a concordance scenario for the $^{13}C(\alpha,n)^{16}O$ S(E)*

# $^{13}C(\alpha,n)^{16}O$-Comparison with Gao+ 2022

Extrapolation to astrophysical energies still needed

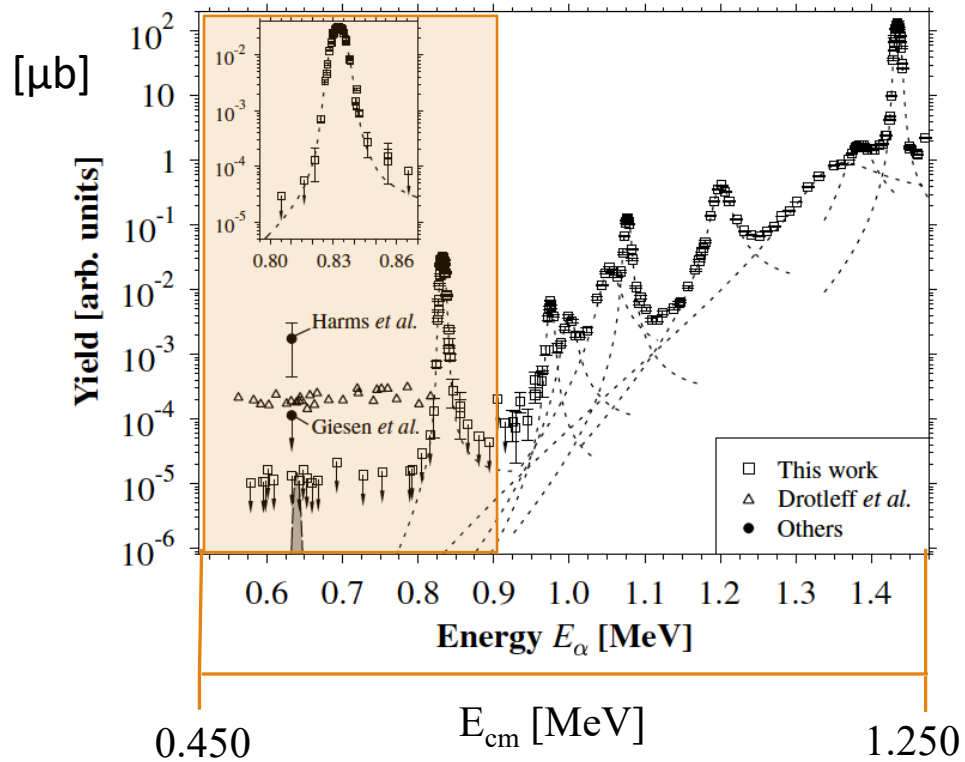Several data sets were not considered in the R-matrix analysis (cherry picking?)

Fail to reproduce the measured ANC of the 6.356 MeV resonance (50% lower)
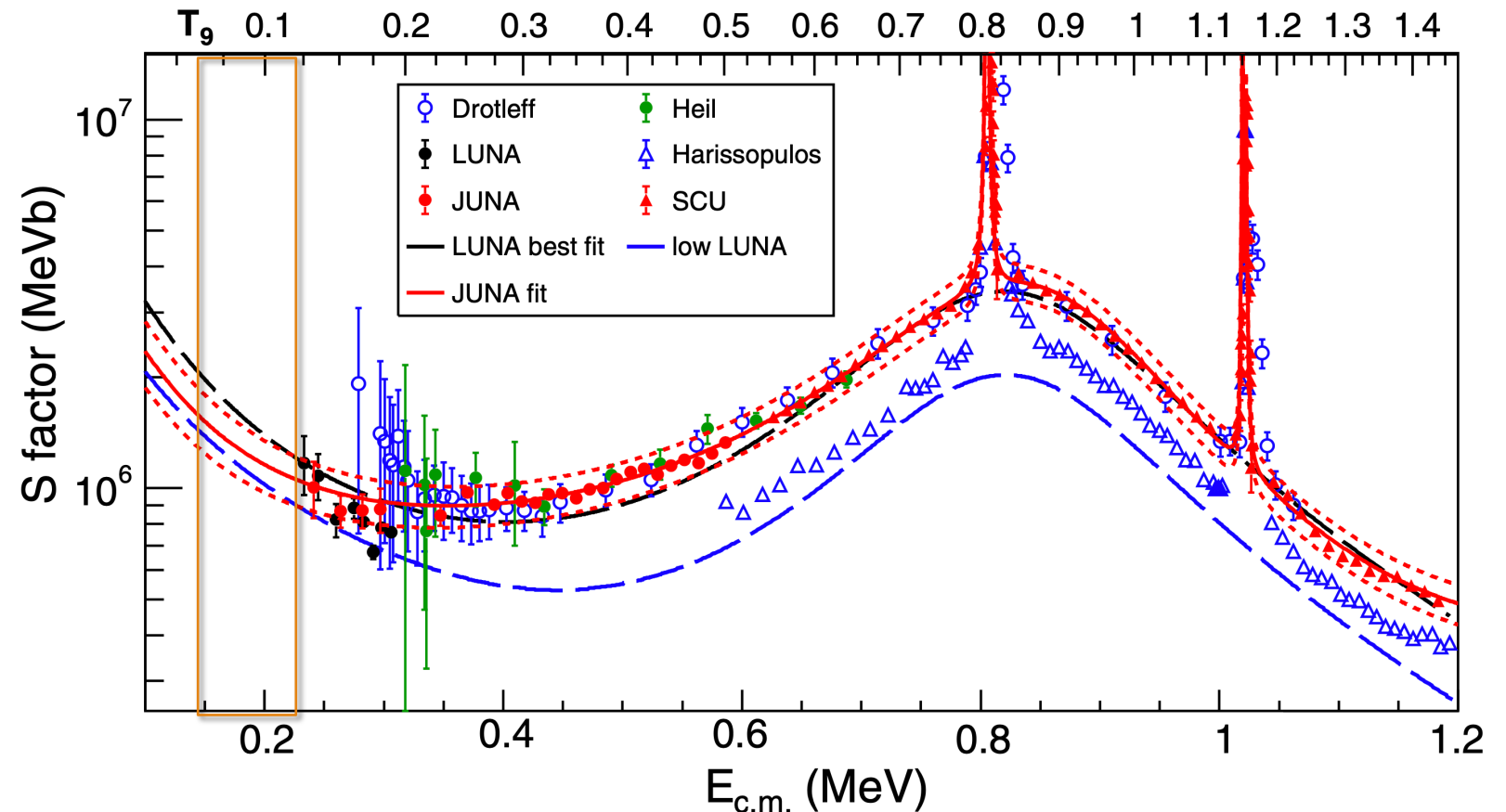
# $^{22}Ne(\alpha,n)^{25}Mg$

# $^{22}$Ne($\alpha$,n)$^{25}$Mg



[Jaeger et al. 2001]

s-process ROI: $E_{cm}$= 600 ± 300 keV (CB@3.5 MeV)
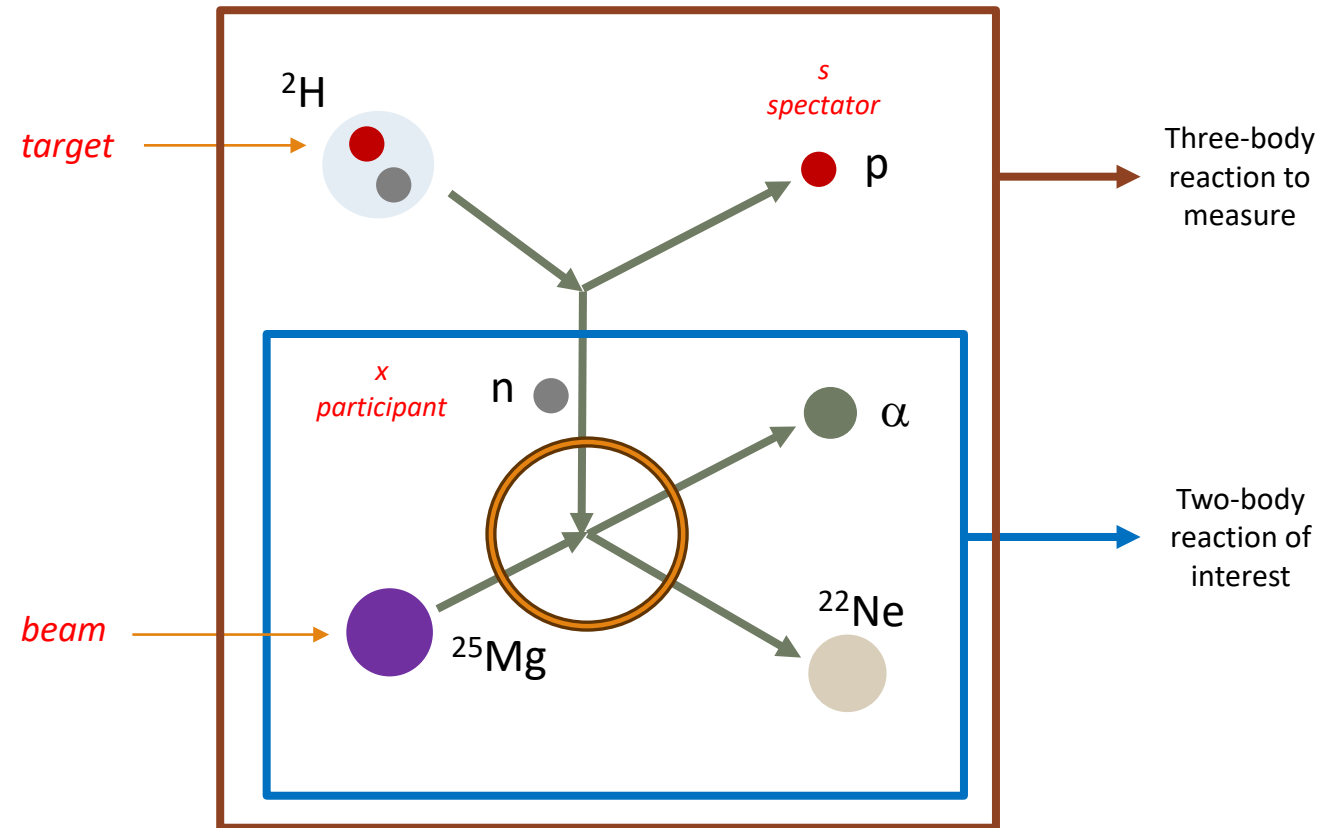
Below 1.2 MeV values are smaller than 1 µb
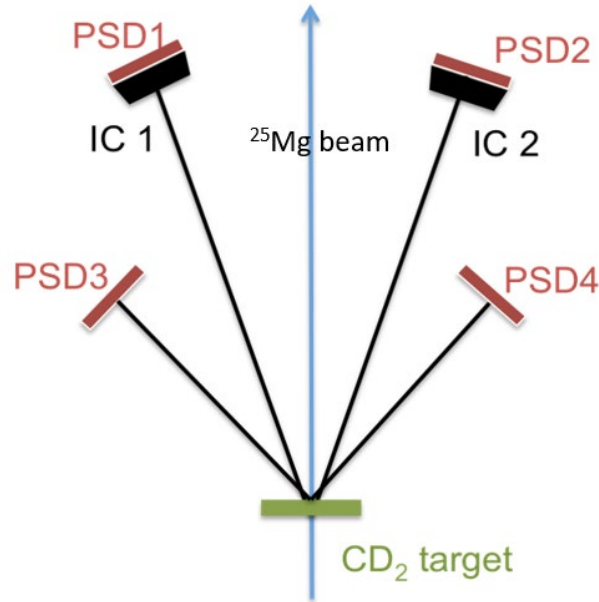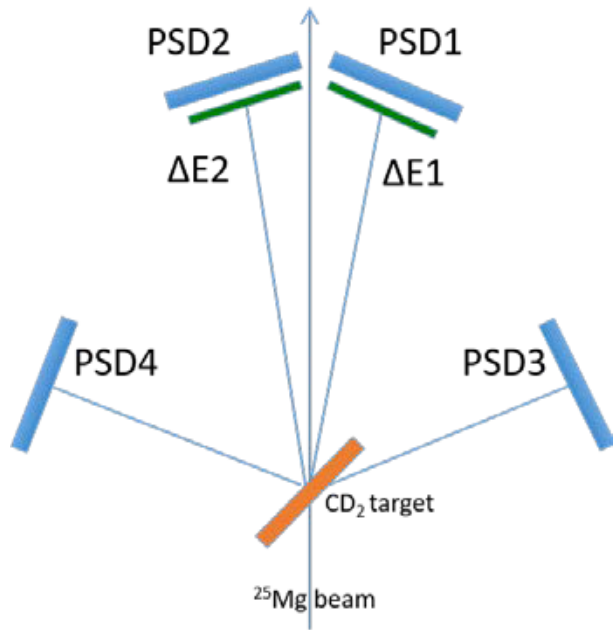→ very difficult to perform direct measurements

Indirect measurement is needed @low energy
to cover the whole range and solve the discrepancy

# $^{22}$Ne($\alpha$,n)$^{25}$Mg

$^{25}$Mg(n,$\alpha$)$^{22}$Ne
+
det.bal.princ.

→ d($^{25}$Mg,n$\alpha$)$^{22}$Ne

# $^{22}Ne(\alpha,n)^{25}Mg$



not worked ?    $^{23}Na$ instead of $^{22}Ne$
$^{26}Mg=^{22}Ne+\alpha$ (*l=0*) ?

1) $\alpha$ - p coincidences. 35 μm as $\Delta E$ stage, but very low $E_{spect-p} < 1$ MeV → threshold to the minimum.

2) $^{22}Ne - \alpha$ coincidence ($\neq E_{beam}$). 2 IC (5 cm deep, $C_4H_{10}$ ) to detect and separate $^{22}Ne$.
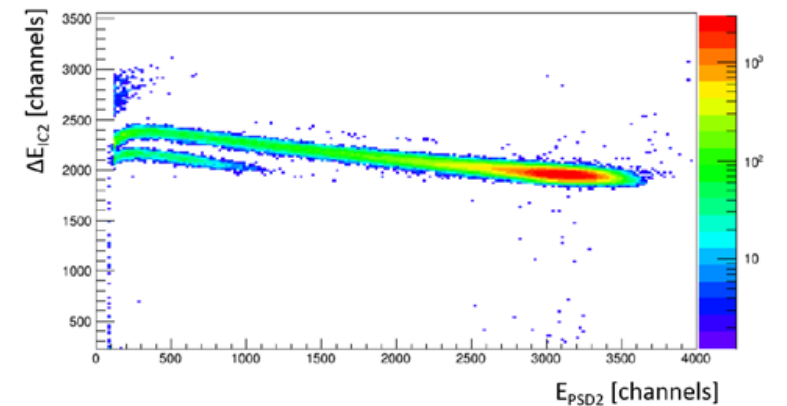
# Conclusions

❑ THM (& ANC) are valid tools to complement the direct measurements results also in the special and crucial context of He-burning.

❑ Indirect methods can help in approaching a concordance scenario.

❑ $^{22}$Ne($\alpha$,n)$^{25}$Mg future TH&direct measurements will be crucial for s-process understanding (TH nuclei tests + $\alpha$ solid targets)

*Thanks for your attention*